Hindawi
Wireless Communications and Mobile Computing
Volume 2020, Article ID 8676835, 11 pages
https://doi.org/10.1155/2020/8676835

Research Article

Transmit Power Allocation with Connectivity Probability for Multi-QoS in Cluster Flight Spacecraft Network

Jinrong Mo[1,2], **Shengbo Hu**[1,2], **Tingting Yan**[1,2], **Xiaowei Song**[1,2] **and Yanfeng Shi**[1,2]

[1]*Institute of Intelligent Information Processing, Guizhou Normal University, Guiyang 550001, China*
[2]*Center for RFID and WSN Engineering, Department of Education Guizhou, Guiyang 550001, China*

Correspondence should be addressed to Jinrong Mo; 935472997@qq.com

Received 19 July 2019; Revised 6 January 2020; Accepted 16 January 2020; Published 17 February 2020

Guest Editor: Dionisis Kandris

In this paper, we investigate the transmit power allocation problem to minimize the average packet error rate at the access point in the cluster flight spacecraft network, which adopts the CSMA/CA channel access mechanism. First, the node mobility, nodal distance distribution, and probabilistic adjacency matrix were formulated for cluster flight spacecraft network based on twin-satellite mode. Then, the optimization-theoretic model described the optimized transmit power allocation strategy and its implementation algorithm was proposed. And the problem of minimizing the packet error rate of the cluster flight spacecraft network system can be converted into maximizing the expectation of the binary probabilistic adjacency matrix, i.e., maximizing the sum of the nondiagonal elements in the probabilistic adjacency matrix. Due to discreteness of nodal distance distribution, Monte Carlo method was applied to solve the transmit power allocation problem. Yet importantly, the influence of node transmit power on the QoS performance of cluster flight spacecraft network was simulated and analyzed under the assumption of finite overall network transmit power and low traffic load. Finally, the results show that the pocket error rate increases with the provided traffic load, but the pocket error rate hardly changes with the same traffic load in different sequential time slots of any orbital hyperperiod or in the same time slot of different orbital hyperperiods, and by maximizing the sum of the nondiagonal elements in the probabilistic adjacency matrix, the pocket error rate minimum is achieved for a given total network transmit power at any time slot for cluster flight spacecraft network.

1. Introduction

In recent years, fractionated spacecraft with cluster flight model has become a hot topic in the field of distributed space network, due to its advantages of flexibility, rapid response, low cost, strong scalability, and long lifetime. The previous work has made a contribution to earth observation and space exploration [1–3]. Fractionated spacecraft distributes the functionality of a traditional large monolithic spacecraft into a number of heterogeneous modules. Each module can be regarded as a node through wireless communication, and the nodes construct the cluster flight spacecraft network (CFSN). Cluster flight spacecraft require mutual cooperation between nodes to realize information exchange, navigation communication, and power sharing. These spacecraft constitute a virtual satellite platform with information exchange structure. In addition, like other distributed space systems, the cluster flight spacecraft is a resource-sharing and energy-limited system. Therefore, how to allocate nodal transmit power efficiently and optimize the performance of the cluster flight spacecraft is an important issue needs to be solved [4–6].

For wireless communication systems, including wireless sensor networks and radar networks, research on optimizing systematic performance by allocating nodal power efficiently has always been a hotspot [7, 8]. For example, in an end-to-end MIMO multihops wireless network with outage probability limited, the power allocation method was studied and the analytic solution of optimal power allocation with the minimum total transmit power of the system was obtained in [9]. Aiming at the problem that it is difficult to obtain an analytic solution for the optimal power allocation in

amplification and forwarding (AF) relay selection of cooperative communication system, artificial neural network was adopted to obtain an efficient solution from the target of minimum bit error rate in [10]. For the cooperative network of spectrum sharing, by solving the convex optimization problem, the optimal power allocation strategy with minimum energy consumption under the requirements of QoS was obtained in [11]. For the symbol programming problem of target detection in distributed radar sensor network, the closed-form expression of optimal power allocation by establishing the optimal linear unbiased estimation model was obtained in [12]. In [13], based on the received signal interference plus noise ratio, Markov chain was adopted to obtain the dynamic power control method with the minimum packet error rate (PER).

To the best of our knowledge, there are few research reports on the optimal power allocation in CFSN. Only the solution of the minimum spanning tree by constructing the spatial-temporal network topology to improve energy efficiency was obtained for the CFSN in [14]. In fact, due to the fact that heterogeneous modules have to meet miscellaneous requirements given different tasks, the CFSN faces the requirements of multi-QoS, including the requirements of different delay and bit error [3]. In general, the resource allocation with multi-QoS, including power, bandwidth, and CPU, is an NP-hard problem in the static network [15, 16]. However, because of the high-speed flight of modules, the topology of the CFSN is highly dynamic and nodes are randomly connected. Therefore, it is foreseeable that the resource allocation with QoS is more complicated in CFSN.

Many researchers have studied the problem of power distribution with multi-QoS in static networks. Among them, based on the resource allocation mode with QoS under the constraint of resource [17], the resource allocation problem with multiresources multi-QoS and single-resource multi-QoS by adopting polynomial concave optimal control method was solved in [15]. By introducing a truncated based on slope, an approximated method of concave optimal control was obtained and the resource allocation problem with multiresources multi-QoS was solved efficiently [16]. In addition, as for radar tracking under the constraints of radar bandwidth, processing time, and transmit power, the method of [16] was adopted to solve the optimization problem of radar tracking and speed accuracy efficiently in [18, 19]. In recent years, with the development of large-scale MIMO technology, the optimization of transmit power allocation has also received widespread attention. For example, the issue of the minimum total transmit power of the system from the perspective of satisfying QoS constraints was studied in [20]. An efficient energy allocation algorithm was studied based on binary search for 5G carrier aggregation scenario in [21]. Under the conditions of given QoS requirements, the optimization of transmit power allocation of full-duplex access core network was studied in [22].

The connection between nodes is the fundamental problem of wireless communication networks. It not only reflects link quality, but also determines network performance. In general, for a static and deterministic network composed of n nodes, the nodes can be denoted as a graph $G(V, E)$, where $V = \{v_1, v_2, \ldots, v_n\}$ denotes the vertex set and E denotes the edge set. The probabilistic adjacency matrix, denoted by A_G, describes the state of the nodal connection and is a symmetric matrix. If there exists an edge between nodes v_i and v_j, $a_{ij} = 1\,(i \neq j)$, otherwise 0, that is, nodes v_i and v_j are not connected [23]. From the perspective of wireless communication, the power of transmitter determines the connection between nodes. Therefore, intuitively, the adjacency matrix A_G directly reflects the transmit power of the system. In this way, based on the probabilistic adjacency matrix, the research on transmit power allocation of wireless communication system is plausible. However, as mentioned above, as the topology of the CFSN is highly dynamic and nodes are randomly connected, we proposed a method of transmit power allocation with multi-QoS by establishing the nodal distance distribution model, defining the binary probabilistic adjacency matrix, and adopting the CSMA/CA channel access mechanism. Our transmit power allocation method is proposed on the following premises: (1) low traffic load, (2) finite overall transmit power, and (3) the star topology of the network, that is, one node is responsible for the earth communication, and others are connected to the node by frequency division multiple access (FDMA) with subcarrier binary phase-shift keying (BPSK) modulation [24]. The purpose of optimal transmit power allocation is to minimize the average PER at the access point (AP) based on the probabilistic adjacency matrix.

The structure of this paper is organized as follows: Section 2 introduces and analyzes the basic model of CFSN and describes the definition of the probabilistic adjacency matrix of this model. In Section 3, the optimization-theoretic model is present. And based on the model, the optimized transmit power allocation strategy is proposed. In Section 4, the simulation results of the PER and delay in the network are presented, focusing on the impact of the probabilistic adjacency matrix, the traffic load, and the adopted power allocation strategy. Finally, Section 5 concludes the paper.

2. System Model

2.1. Definition of a Simplified Model in CFSN. The link connection characteristics between nodes in CFSN depend on the relative orbits, transmit power, and receiving sensitivity of the nodes. Therefore, the following definition is given:

Definition 1. In ECI coordinates [24, 25], for each time slot in an orbital hyperperiod of CFSN, a node can be defined as a couple $s = (x, P)$, where $x \in R^3$ is the location of node and $P \in R$ is its transmit power.

Given a spacecraft network consisting of L nodes with interference limited, if node $s_j = (x_j, P_{tj})$ can receive the signal transmitted by the node $s_i = (x_i, P_{ti})$, the bit-signal-to-noise ratio at the receiving node s_j should satisfy the following equation:

$$\frac{E_b}{N_0} = \frac{P_{ti}G_tG_r\lambda^2}{(4\pi)^2\left\|x_i - x_j\right\|^2 kTR_b} \geq \Gamma, \tag{1}$$

where N_0 is the additive white noise power spectral density of receiver, k is Boltzmann's constant, T is the noise temperature, P_{ti} is the transmit power of node s_i, $\|x_i - x_j\|$ is the Euclidean distance between s_i and s_j, R_b is the rate of data transmission, G_{ti} and G_{rj} are the gains of the transmit and receive antennas, λ is the working wavelength, and Γ is the receiving sensitivity and depends on the modulation mode, etc. For QPSK modulation, when the bit error rate is less than 10^{-5}, $\Gamma = 9.6$ dB. In order to facilitate the calculation, it can be assumed that $G_{ti} = G_{rj} = 1$.

In CFSN, $m \leq \|x_i - x_j\| \leq M$, M and m are the upper bound and the lower bound of nodal distance, respectively [24].

Therefore, equation (1) can be simplified as follows:

$$\left\|x_i - x_j\right\|^2 \leq \frac{P_{ti}\lambda^2}{(4\pi)^2 kTR_b\Gamma}. \tag{2}$$

According to the following equation, the distance threshold of any successful connection between s_i and s_j can be obtained:

$$d_\Gamma = \sqrt{\frac{P_{ti}\lambda^2}{(4\pi)^2 kTR_b\Gamma}}, \quad m \leq d_\Gamma \leq M. \tag{3}$$

That is, if $\|x_i - x_j\| \leq d_\Gamma$, then s_i and s_j are connected to each other. And we can derive from equation (3):

$$m^2\frac{(4\pi)^2 kTR_b\Gamma}{\lambda^2} \leq P_{ti} \leq M^2\frac{(4\pi)^2 kTR_b\Gamma}{\lambda^2}. \tag{4}$$

Therefore, the network can be defined as follows:

Definition 2. A CFSN of L nodes, in each time slot of its orbital hyperperiod, can be defined as an order set: $S = (s_{\mathrm{AP}}, d_\Gamma, s_1, s_2, \ldots, s_L)$, where $s_{\mathrm{AP}} \in R^3$ is the location of the AP.

Based on Definition 2, the definition of binary adjacency matrix in CFSN can be obtained.

Definition 3. For a given CFSN $S = (s_{\mathrm{AP}}, d_\Gamma, s_1, s_2, \ldots, s_L)$, in each time slot of its orbital hyperperiod, the binary adjacency matrix is given by $A(S) \in R^{L\times L}$, where

$$A_{ij} = A(S)_{ij} = \begin{cases} 1, & \left\|x_i - x_j\right\| \leq d_\Gamma, \\ 0, & \text{otherwise.} \end{cases} \tag{5}$$

And the complement of $A(S)$ corresponds to

$$\overline{A}(S) = \begin{cases} 1, & A_{ij} = 0, \\ 0, & \text{otherwise.} \end{cases} \tag{6}$$

To simplify the calculation, the number of ones in the adjacency matrix is denoted by $|A(S)|$, and the complementary adjacency is given by the number of zeros in adjacency matrix, denoted by $|\overline{A}(S)|$.

Moreover, for the sake of analysis, for $i = 1, 2, \ldots, L$, two index sets of nodes are defined: $R_i = \{j = 1, \ldots, L \mid A_{ji} = 1\}$ and $T_i = \{j = 1, \ldots, L \mid A_{ij} = 1\}$. They represent the node index that node s_i can receive from and transmit to, respectively.

2.2. Nodal Mobility Model and Distance Distributions in CFSN. To accomplish the cluster flight model within bounded distance, twin-satellite mode was adopted to study the nodal mobility model. The node position is uniformly distributed on sphere within $(M - m)/4$ radius as shown in Figure 1.

So the mobility model $M(t)$ within bounded distance for CFSN can be defined as follows.

Definition 4. In ECI coordinates, if the position sets of n nodes in CFSN are $\mathbf{R}(0) = \{\mathbf{r}_1(0), \mathbf{r}_2(0), \ldots, \mathbf{r}_n(0)\}$ at initial time T_0, the position set is $\mathbf{R}(k) = \{\mathbf{r}_1(k), \mathbf{r}_2(k), \ldots, \mathbf{r}_n(k)\}$, and the positions are uniformly distributed within sphere $B(\mathbf{r}_i(0), a)$ $(i = 1, 2, \ldots, n)$ at time T_k, where $\mathbf{r}_i(0)$ and $a = ((M - m)/4)$ are center and radius of the sphere, respectively. Moreover, positions among all nodes are mutually independent and independent of all previous locations.

Based on the nodal mobility model, the nodal distance distribution can be described in Figure 2. Nodes are assumed to be uniformly located in a circle of the two-dimensional plane.

In Figure 2, the coordinates of the transmitter A and the receiver B are $(r_A\cos\varphi_A\varphi, r_A\sin\varphi_A)$ and $(D + r_B\cos\varphi_B, r_B\sin\varphi_B)$, respectively, where, $r_A, r_B \in [0, a]$ and $\varphi_A, \varphi_B \in [0, 2\pi]$, and D with the value $(M + m)/2$ is the distance between the centers of the two circle. The random variables with probability density functions are given by

$$f_{r_{A,B}}(r_{A,B}) = \begin{cases} \dfrac{2r_{A,B}}{a^2}, & 0 \leq r_{A,B} \leq a, \\ 0, & \text{otherwise,} \end{cases}$$
$$f_{\varphi_{A,B}}(\varphi_{A,B}) = U(0, 2\pi), \tag{7}$$

where $U(0, 2\pi)$ is the uniform distribution over range $[0, 2\pi)$, and the subscripts denote r_A, r_B and φ_A, φ_B, respectively.

Therefore, the distance between the transmitter A and the receiver B is given by

$$\|AB\| = \sqrt{(r_A\cos\varphi_A - (D + r_B\cos\varphi_B))^2 + (r_A\sin\varphi_A - r_B\sin\varphi_B)^2}. \tag{8}$$

Despite the simplicity of equation (8), the derivation of the distance density cannot be given in closed form. According to Glivenko–Cantelli Lemma, adopting empirical statistical method and eighth-order polynomial approximation, the probability density function of the distance between nodes with eighth-order polynomial can be denoted by

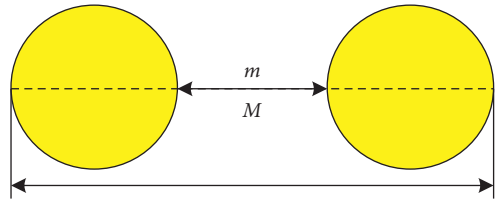

Figure 1: Nodal mobility model.

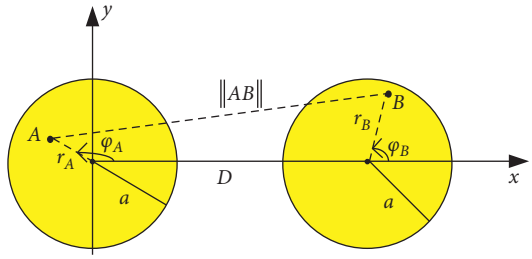

Figure 2: Nodal distance distribution.

$$\hat{f}_8(h) \approx \begin{cases} \sum_{i=0}^{8} p_i h^i, & \frac{m}{D} \le h \le \frac{M}{D}, \\ 0, & \text{otherwise.} \end{cases} \tag{9}$$

When $m = 2.5$ km and $M = 90.1$ km, the polynomial coefficients of the empirical probability density function are provided in Table 1.

2.3. Determination of Probabilistic Adjacency Matrix in CFSN. According to the foregoing, the definition of the probabilistic adjacency matrix for CFSN is described as follows.

Definition 5. Given the CFSN $S = (s_{AP}, d_\Gamma, s_1, s_2, \ldots, s_L)$, in each time slot of an orbital hyperperiod, the probabilistic adjacency matrix is a $L \times L$ matrix. p_{ij} is the (i, j) element, and $p_{ij} = p_{ji}$. p_{ij} is the probability that s_i and s_j successfully connect. The diagonal entries are all equal to 1.

Because the satellite has the capability of storage and forwarding, the diagonal entries are all equal to 1.

If $d = \|x_i - x_j\|$, the connectivity probability between s_i and s_j is given by

$$p_{ij} = \Pr\{d = d_{ij} \mid d < d_\Gamma\}. \tag{10}$$

3. Packet Error Rate, Transmission Delay, and Power Optimization of the System

In order to analyze the relationship between the system's PER, transmission delay, and the probabilistic adjacent matrix, the following two counting processes [26] are assumed: in the time interval $(0, t)$, the number of times that packet transmission of other nodes has been checked by node i is a homogeneous Poisson process G_i with intensity g (dimension: pck/s), and the number of times that a node i has transmitted packet is also a homogeneous Poisson process $T_i(t)$ with intensity g. Besides, the processes associated with different nodes are independent of each other, all data can be transmitted successfully within $(0, t)$, and the data transmission length is $T_{\text{trans}} = B_L/R$, where B_L is the packet length (dimension: b/pck) and R is the transmission data rate (dimension: b/s).

Table 1: Coefficients of the fitting polynomials.

p_i	
p_0	0.0872
p_1	−0.7380
p_2	2.5135
p_3	−4.3913
p_4	4.1737
p_5	−2.1499
p_6	0.5919
p_7	−0.0764
p_8	0.0034

3.1. Packet Error Rate and Delay of the System

3.1.1. Packet Error Rate. For a certain time slot in the orbital hyperperiod of CFSN, if only the adjacency matrix is taken into account, the bidirectional packet error intensity accumulated by node i will be

$$F[E_i] = \gamma_i F[G_i] + \lambda_i F[T_i], \tag{11}$$

where $\gamma_i F[G_i]$ represents the intensity of transmission errors that s_i cannot receive the packet because the nodes are not connected. $\lambda_i F[T_i]$ represents the intensity of transmission errors due to interference from other nodes that cannot receive s_i.

When the system has low traffic load, i.e., $gT_{\text{trans}} << 1$, the coefficients γ_i and λ_i in equation (11) can be expressed, respectively, as follows:

$$\begin{aligned} \gamma_i &= \lim_{t \to \infty} P\left\{ \max_{j \in \overline{R}_i} \{T_j[t + T_{\text{trans}}] - T_j[t]\} > 0 \right\} \\ &= 1 - \prod_{j \in \overline{R}_i} \left(1 - e^{-F[T_j]T_{\text{trans}}}\right) \approx \sum_{j \in \overline{R}} F[T_j] T_{\text{trans}} = |\overline{R}_i| T_{\text{trans}} g, \end{aligned} \tag{12}$$

$$\begin{aligned} \lambda_i &= \lim_{t \to \infty} P\left\{ \max_{j \in \overline{G}_i} \{G_j[t + T_{\text{trans}}] - G_j[t]\} > 0 \right\} \\ &= 1 - \prod_{j \in \overline{T}_i} \left(1 - e^{-F[G_j]T_{\text{trans}}}\right) \approx \sum_{j \in \overline{T}_j} F[G_j] T_{\text{trans}} = |\overline{T}_i| T_{\text{trans}} g. \end{aligned} \tag{13}$$

Using the expressions above for coefficients γ_i and λ_i in (12) and (13), the transmission error intensity of node i is given by

$$F[E_i] = \mathbb{E}\left[\left(|\overline{T}_j| + |\overline{R}_i|\right)\right] T_{\text{trans}} g^2, \tag{14}$$

where $\mathbb{E}[\cdot]$ denotes the expected value. Therefore, the overall network error intensity is given by

$$\sum_{i=1}^{L} F[E_i] = 2\mathbb{E}[|\overline{A}(S)|]T_{\text{trans}}g^2. \tag{15}$$

According to the previous assumption, the overall network intensity is g, so the probability of packet error, i.e., the ratio between the overall network error intensity and the generation intensity (given by Lg), is as follows:

$$P_{\text{er}} = \frac{\sum_{i=1}^{L} F[E_i]}{Lg} = \frac{2\mathbb{E}[|\overline{A}(S)|]T_{\text{trans}}g}{L}. \tag{16}$$

3.1.2. Transmission Delay. In order to analyze the relation between transmission delay and probabilistic adjacency matrix, the CSMA/CA mechanism is assumed to be adopted for the node access in CFSN. If the channel idle assessment time is T_{CCA}, and the access back-off time of the busy channel is T_B, the transmission delay connecting node i that can receive the data packet is as follows:

$$\begin{aligned} D_i &= (T_{\text{CCA}} + T_B) \sum_{j \in \mathscr{R}_i} F[T_j] T_{\text{trans}} \\ &\approx (T_{\text{CCA}} + T_B)\mathbb{E}[\mathscr{R}_i] g T_{\text{trans}}. \end{aligned} \tag{17}$$

Therefore, the average transmission delay of CFSN can be estimated as follows:

$$\overline{D} = \frac{\sum_{i=1}^{L} D_i}{L} \approx (T_{CCA} + T_B)\frac{\mathbb{E}[|A(S)|]}{L} T_{\text{trans}} g. \tag{18}$$

3.2. Optimal Transmit Power Allocation. The purpose of the transmit power allocation is to optimize the QoS of the CFSN system. It can be seen from equation (14) that the problem of optimizing the transmit power allocation for minimizing the PER of the CFSN system is equivalent to maximizing $\mathbb{E}[|A(S)|]$, i.e., maximizing the sum of the nondiagonal elements in the probabilistic adjacency matrix.

If $\mathscr{P} = [0.0002, 0.25]$, and total power of CFSN system is P_{tot}, the discrete optimization problems can be formulated as follows.

Problem. For a given CFSN $S = (s_{\text{AP}}, d_\Gamma, s_1, s_2, \ldots, s_L)$, in each time slot of its orbital hyperperiod, each node chooses a transmit power $P_{ti} \in \mathscr{P}$ $(i = 1, \ldots, L)$, and the transmit power allocation with the smallest PER needs be optimized as follows:

$$\begin{aligned} &\max \quad \mathbb{E}[|A(S)|] \\ &\text{s.t.} \quad \sum_{i=1}^{L} P_{ti} \le P_{\text{tot}}. \end{aligned} \tag{19}$$

Using the conditional probability method, (10) can be rewritten as

$$p_{ij} = \frac{\Pr\{d = d_{ij}\}}{\Pr\{d < d_\Gamma\}}. \tag{20}$$

Substituting (20) to (19), because maximizing $\mathbb{E}[|A(S)|]$ is equivalent to maximizing the sum of the nondiagonal elements in the probabilistic adjacency matrix, the optimization problem can be converted into

$$\begin{aligned} &\max \quad \sum_{i=1}^{L} \sum_{j=1, j\neq i}^{L} \frac{\Pr\{d = d_{ij}\}}{\Pr\{d < d_\Gamma\}} \\ &\text{s.t.} \quad C1\text{: } \sum_{i=1}^{L} P_{ti} \le P_{\text{tot}} \\ &\qquad C2\text{: } d_{ij} < d_\Gamma. \end{aligned} \tag{21}$$

The constraint $C1$ and $C2$ denote that the total network transmit power is finite and the distance between connected nodes is within the threshold of node s_i and s_j. Since $d_{ij} = \sqrt{(P_{ti}\lambda^2)/((4\pi)^2 kTR_b\Gamma)}$, the nonconvexity of constraint $C2$ can be proved by the second-order partial derivative with respect to the variable.

It is noted that equation (21) is a nonlinear multichoice knapsack problem, which can be solved by Monte Carlo method [27, 28]. Moreover, it is also noted from equations (16) and (18) that the PER and the average delay of the system are linear with $\mathbb{E}[|A(S)|]$.

The outline of the power allocation algorithm is given as follows.

Step 1: initialization: set $B_L = 632$, $R = 1 \times 10^5$, $T_{\text{CCA}} = 128 \times 10^{-6}$, $T_B = 320 \times 10^{-6}$, $L = 5$, $P_{\text{tot}} = 0.65$, $0 \le \sum_{i=1}^{L} P_{\text{ti}} \le P_{\text{tot}}$.

Step 2: set $k = 1$, and choose a large value for N, where: $k = 1$, $N =$ total number of trials.

Step 3: generate a uniformly distributed random transmit power for each node, $RN = 0.0002 + 0.2498 \times \text{rand}(1, L)$ (using MATLAB, $\text{rand}(X, Y)$ denotes a $X \times Y$ matrix where its elements range from 0 to 1. In this paper, the transmit power for each node is $P_{ti} \in \mathscr{P}$, so RN can be computed by mapping $\text{rand}(1, L)$).

Step 4: calculate the probability of the AP received from node j $(i = \text{AP}, j \neq i)$: compute the transmit distance threshold from node i to AP using equation (3), and compute the connectivity probability of this link using equation (21).

Step 5: calculate the probability of the AP transmitted to node j $(i = \text{AP}, \quad j \neq i)$: compute the transmit distance threshold from AP to node i using equation (3), and compute the connectivity probability of this link by using equation (21).

Step 6: sum the connectivity probability of Step 4 and Step 5.

Step 7: add 1 to k, if $k > N$, calculate the max sum of Step 6 and end; otherwise, go to Step 3.

NOTE: Monte Carlo algorithm means that the more the samples, the more approximate the optimal value

[29]. As $N \longrightarrow \infty$, the objective value tends to the optimal solution.

4. Simulation Analysis

In order to simulate and analyze the influence of node transmit power on the QoS performance of CFSN, packet error rate, average delay, and two allocation strategies are considered: (1) each node has the same transmit power and (2) the optimal transmit power varies from node to node and is allocated using strategy presented in Section 3.2.

The simulations have been carried out referring to star topology, i.e., all nodes transmit (receive) directly to (from) the AP, and using different values of the overall network transmit power and, consequently, different values of the transmit powers allocated to the spacecraft. Simulation parameter settings are as follows: (1) transmit power. It is assumed that the module used to collect solar panels is powered by microwave wireless power transfer to other modules, and each module provides an effective total power of 0.13 W [24]. (2) The number of nodes of the cluster flight spacecraft $L1 = 5$ and $L2 = 7$, and the orbital elements are derived from [24]. (3) The noise temperature is 300 K. The QPSK modulation is adopted between nodes. The transmission data rate is 100 kbps, the operating frequency is S-band, and $f = 2.2$ GHz [30]. The gains of the transmit and receive antennas are 1 [31]. Other parameters are listed in Table 2 and one considered topology with $L1 = 5$ is shown in Figure 3.

Table 2: Parameter setting.

Parameter	Value
Γ	9.6 dB
P_{tot}	0.65 W
m	2.5 km
M	90.1 km

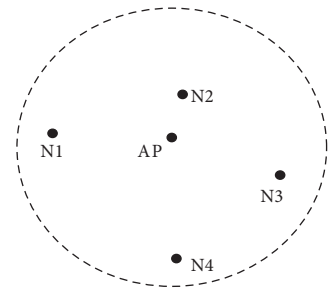

Figure 3: One considered CFSN topology with $L = 5$.

4.1. Each Node with the Same Transmit Power

4.1.1. Impact of the Traffic Load on PER. According to STK and MATLAB simulation, the nodal distance between AP and other nodes can be listed in Tables 3 and 4. Tables 3 and 4 show that the distance between AP and other nodes changes slowly in different time slots of an orbital hyperperiod, and the distance also has a slight change in corresponding time slots of different orbital hyperperiods.

Since the transmit power of each node is the same, it can be assigned to $P_{t1} = P_{t2} = \cdots = P_{t5} = P_{t6} = P_{t7} = 0.13 \quad W$ by equation (4), and the value satisfies all the constraints. The PER is shown as a function of the offered traffic load g in CFSN. Comparing the first, the second, and the third time slots in an orbital hyperperiod, the PER hardly changes. The simulation curves are almost overlapping, as shown in Figure 4. Because the change of the distance is not obvious, the probability of connection between nodes has small change in different sequential time slots of any orbital hyperperiod. Comparing the first and the second orbital hyperperiod in a time slot, the phenomenon in Figure 5 is the same as Figure 4. The reason is that the probability of connection between nodes has a slight change in corresponding time slots of different hyperperiods, and the PER is likely to change periodically.

In order to verify the impacts of different transmit power on PER, the same transmit power is allocated to each node with different values in the first time slot. The result is shown in Figure 6. Comparing the curves referring to each node with 0.13 W, each node with 0.08 W with referring to each node with 0.03 W, it can be concluded that if the transmit power is higher, the PER will be lower under the satisfied constraints. As shown in Figures 4–6, the PER increases with the offered traffic load. In other words, when the traffic load is low, the number of collisions at the AP is likely to be low. Instead, when the traffic load is lager, the probability that two nodes transmit at the same time increases and, subsequently, the PER increases as well.

Keeping other parameters unchanged, the PER under two cases of different numbers of nodes was analyzed. As shown in (b) of Figures 4–6, the PER also increases with the offered traffic load. Comparing (a) and (b) of Figures 4–6, it can be further obtained that the number of nodes increases in the network and the PER increases.

4.1.2. Impact of Each Time Slot $\mathbb{E}[|A(S)|]$ on PER and Delay. According to the analytical results in Section 3.2, the performance, in terms of PER, depends only on the adjacency matrix. For this scenario, the packet generation rate is set to $g = 1$ pck/s. We consider the first time slot of the first orbital hyperperiod in CSFN. Figure 7 shows the impact of $\mathbb{E}[|A(S)|]$ on PER and delay. When the number of nodes increases, the dimension of the adjacency matrix increases, which in turn affects $\mathbb{E}[|A(S)|]$. The dotted line and solid line indicate 7 nodes and 5 nodes, respectively. The results show that the larger the $\mathbb{E}[|A(S)|]$ becomes, the lower the PER will be, and the lager the delay will be. However, the PER and the delay increase with the number of nodes.

4.2. Optimal Transmit Power Allocation Strategy. In this section, we present the impact of the adopted transmit power allocation strategy on the PER of CFSN. In particular,

Table 3: The nodal distance between AP and other nodes ($L1 = 5$) (km).

	Nodal distance	AP to node 1	AP to node 2	AP to node 3	AP to node 4
The first orbital hyperperiod	Time slot 1	5.233	13.748	45.049	53.210
	Time slot 2	4.897	14.446	46.426	55.118
	Time slot 3	4.568	15.177	47.798	57.036
The second orbital hyperperiod	Time slot 1	4.812	14.629	46.762	55.607
	Time slot 2	4.485	15.367	48.131	57.526
	Time slot 3	4.171	16.129	49.486	59.442

Table 4: The nodal distance between AP and other nodes ($L2 = 7$) (km).

	Nodal distance	AP to node 1	AP to node 2	AP to node 3	AP to node 4	AP to node 5	AP to node 6
The first orbital hyperperiod	Time slot 1	7.724	19.582	28.159	53.190	29.171	49.567
	Time slot 2	8.052	20.406	29.380	55.091	30.010	51.422
	Time slot 3	8.385	21.243	30.621	57.002	30.851	53.267
The second orbital hyperperiod	Time slot 1	8.137	20.614	29.694	55.584	30.219	51.900
	Time slot 2	8.471	21.452	30.940	57.496	31.060	53.740
	Time slot 3	8.807	22.296	32.196	59.405	31.900	55.561

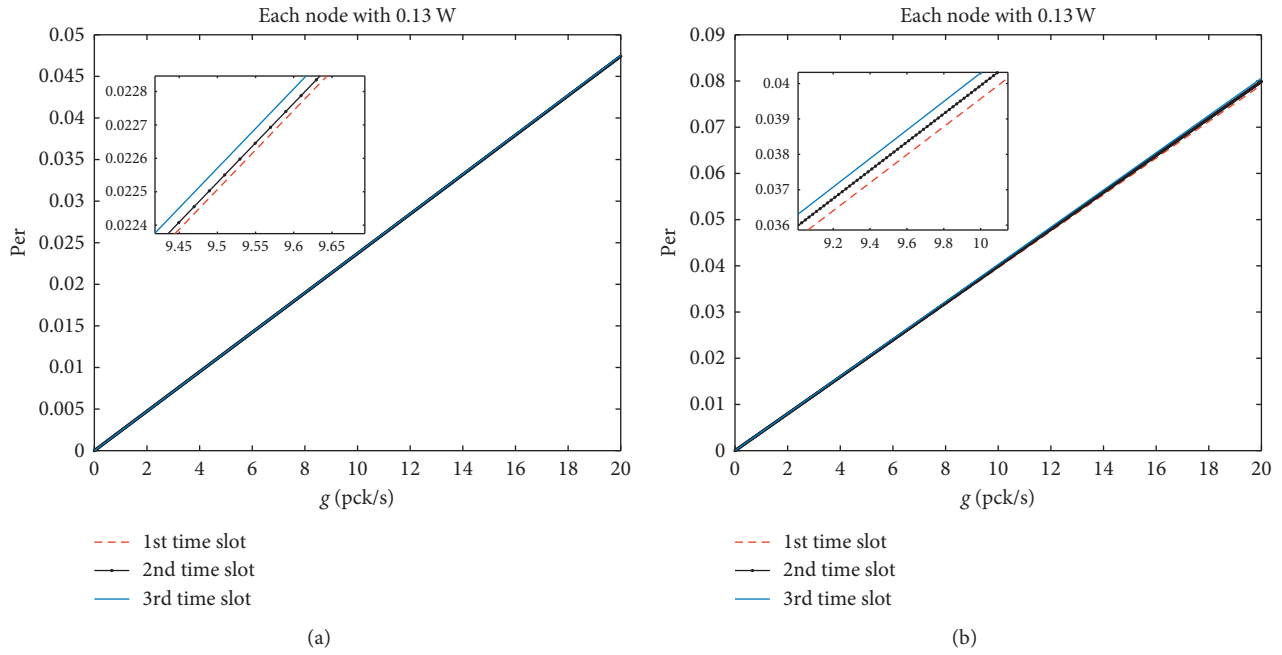

Figure 4: PER as a function of the offered traffic load g in different time slots with the same transmit power. (a) $L1 = 5$. (b) $L2 = 7$.

we consider strategies such that optimized and uniformly distributed transmit power is allocated to each node. The optimized transmit power is different at each node and is set according to the power allocation algorithm presented in Section 3.2, where the total transmit power is assigned to each node in order to minimize the PER in the CFSN. This method leads to allocating transmit power reasonably.

Figure 8 shows the impacts of optimized and uniformly distributed transmit power on PER in the first time slot of the first orbital hyperperiod in CSFN. Different values of total network transmit power are considered. Under the transmit power allocation strategy presented in Section 3.2, in Figure 8, a performance comparison between scenarios with and without the use of the proposed transmit power allocation strategy is presented. Comparing the curves referring to $P_{tot} = 0.65$ W with referring to $P_{tot} = 0.5$ W, it can be concluded that if the total transmit power is higher, the sum of the nondiagonal elements in the probabilistic adjacency matrix will be larger and the PER will be lower under the satisfied constraints. Comparing (a) and (b) of Figure 8, it can be concluded that the increment in the number of

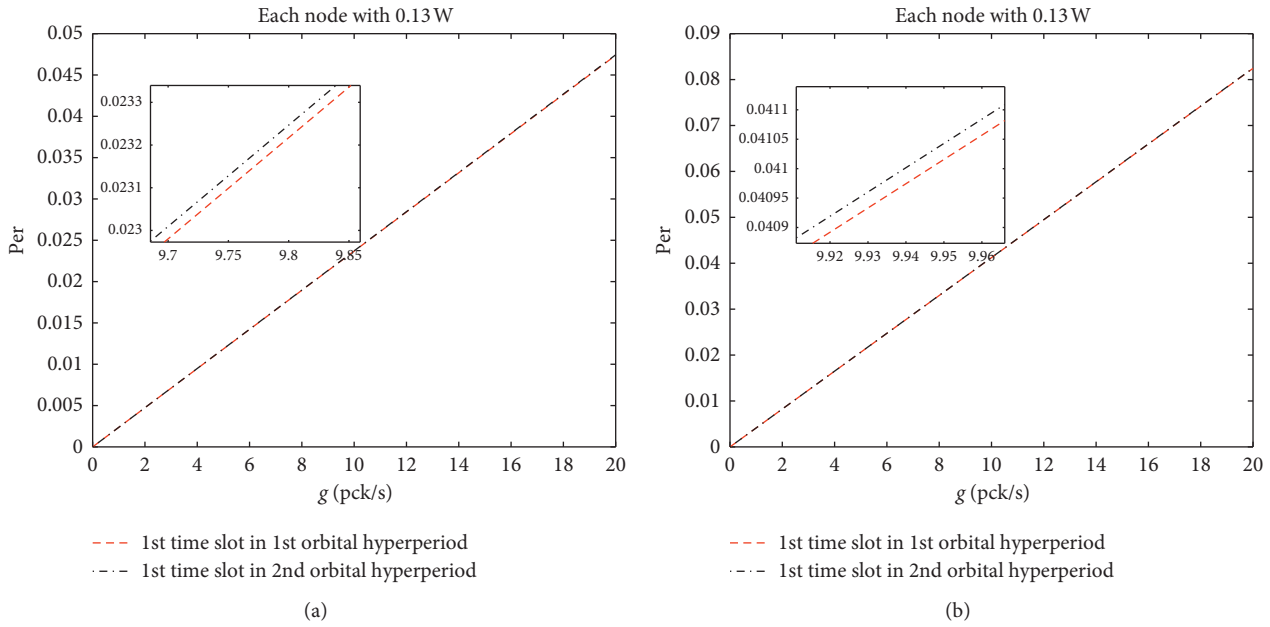

FIGURE 5: PER as a function of the offered traffic load g in the 1st time slots of different orbital hyperperiods with the same transmit power. (a) $L1 = 5$. (b) $L2 = 7$.

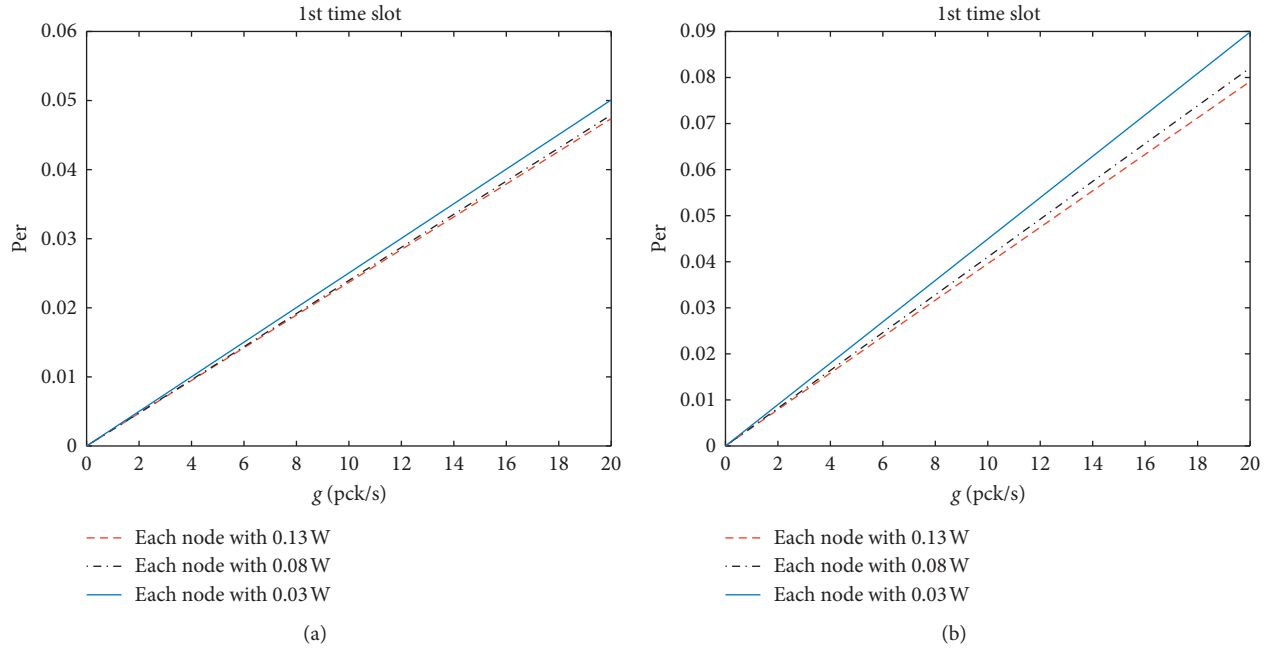

FIGURE 6: PER as a function of the offered traffic load g in a time slot with different transmit power. (a) $L1 = 5$. (b) $L2 = 7$.

nodes will increase the PER of the system. For the sake of comparison, in Figure 8, the PER in scenarios where no transmit power allocation strategy is used (solid line) is also shown. In this case, the performance is worse than the case with the optimized transmit power allocation strategy. In fact, given a value of total network transmit power, the proposed transmit power allocation strategy allows to maximize the sum of the nondiagonal elements in the probabilistic adjacency matrix and, therefore, reduce the PER.

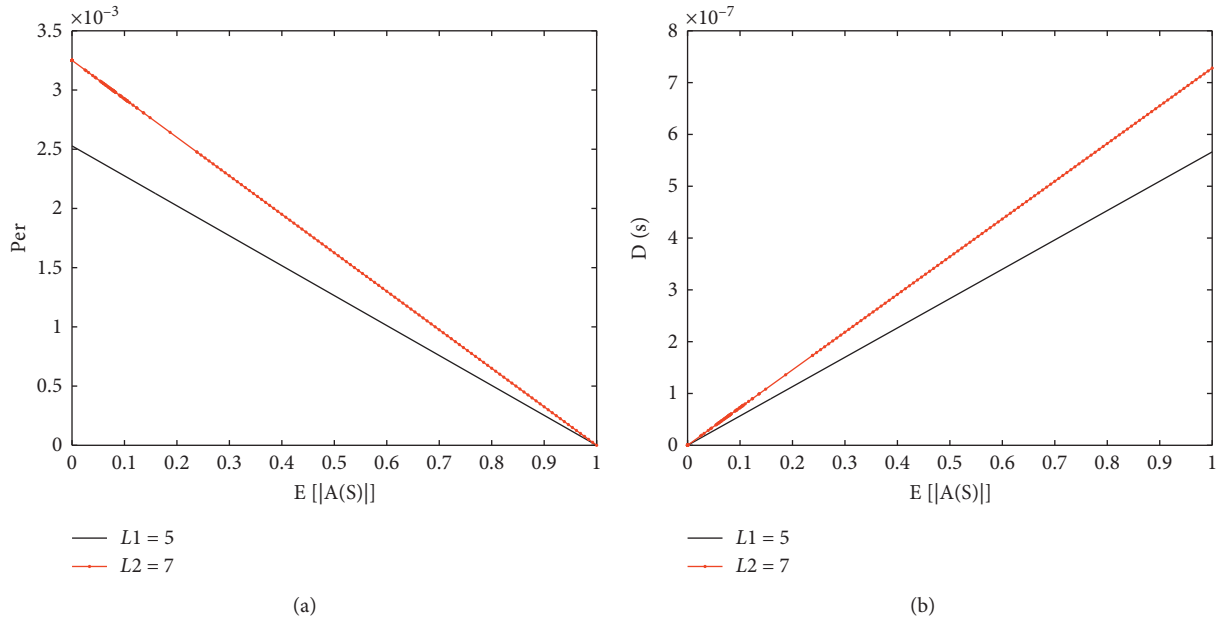

Figure 7: PER and delay as a function of the $\mathbb{E}[|A(S)|]$. (a) PER. (b) Delay.

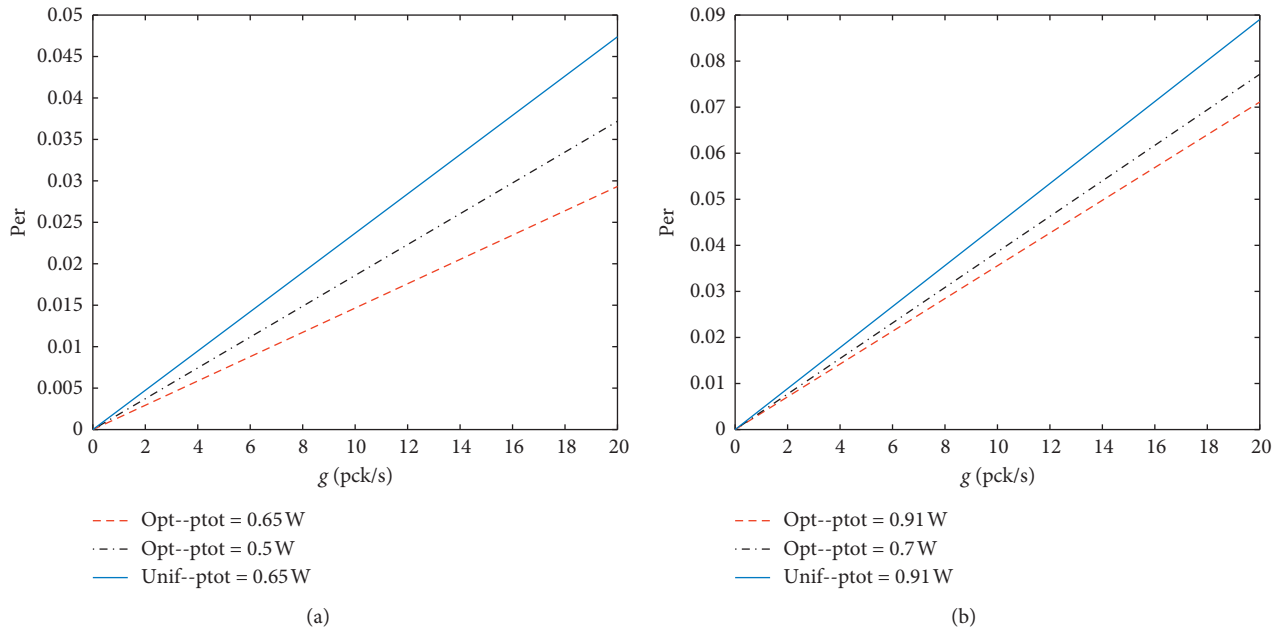

Figure 8: PER as a function of the offered traffic load g in the 1st time slot. (a) $L1 = 5$. (b) $L2 = 7$.

5. Conclusion

In this paper, we have presented an optimized transmit power allocation strategy which allows to minimize the PER of CFSN. First, according to the probabilistic adjacency matrix, we have derived a simplified analytical model which describes the performance of CFSN in different time slots, under the assumption of offered traffic load. Then, we have presented optimization-theoretic transmit power allocation algorithm and implemented it under the assumption of finite total network transmit power under two cases of different numbers of nodes. In particular, we have shown the performance depends on the probabilistic adjacency matrix: the sum of the nondiagonal elements and traffic load. Our analytical model has been validated through the Monte Carlo method. This paper has presented the impact of the probabilistic adjacency matrix, the offered traffic load, and transmit power allocation strategy on relevant network performance indicators (PER and delay). Finally, we have verified that the proposed transmit power allocation

strategy, by maximizing the sum of the nondiagonal elements in the probabilistic adjacency matrix, allows to minimize the PER for a given total network transmit power at any time slot for CFSN.

Data Availability

The orbital data of CFSN composed of 5 satellites and 7 satellites that used to support the findings of this study are included within the article and from literature [24].

Conflicts of Interest

The authors declare that there are no conflicts of interest.

Acknowledgments

This research is a project partially supported by the National Natural Science Foundation of China (Grant no. 61362004) and Guizhou Provincial Education Innovation Group Foundation (Grant no. [2017] 031).

References

[1] L. Mazal and P. Gurfil, "Cluster flight algorithms for disaggregated satellites," *Journal of Guidance, Control, and Dynamics*, vol. 36, no. 1, pp. 124–135, 2013.

[2] S. Nag, C. K. Gatebe, and O. d. Weck, "Observing system simulations for small satellite formations estimating bidirectional reflectance," *International Journal of Applied Earth Observation and Geoinformation*, vol. 43, no. 2, pp. 102–118, 2015.

[3] A. Kandhalu and R. Rajkumar, "QoS-based resource allocation for next-generation spacecraft networks," in *Proceedings of the IEEE 33rd Real Time Systems Symposium*, pp. 1052–8725, San Juan, Puerto Rico, December 2012.

[4] I. del Portillo, E. Bou, E. Alarcon et al., "On scalability of fractionated satellite network architectures," in *Proceedings of the IEEE Aerospace Conference*, pp. 1–13, Big Sky, MT, USA, March 2015.

[5] J. Du, C. Jiang, J. Wang et al., "Resource allocation in space multiaccess systems," *IEEE Transactions on Aerospace and Electronic Systems*, vol. 53, no. 2, pp. 598–618, 2017.

[6] O. Brown, P. Eremenko, and M. Bille, "Fractionated space architectures: tracing the path to reality," 2009, https://digitalcommons.usu.edu/smallsat/2009/all2009/2/.

[7] F. Wand, H. Xing, and J. Xu, "Optimal resource allocation for wireless powered mobile edge computing with dynamic task arrival," in *Proceedings of the IEEE International Conference on Communications*, Shanghai, China, May 2019.

[8] K. Long, P. Wang, W. Li, and D. Chen, "Spectrum resource and power allocation with adaptive proportional fair user pairing for NOMA systems," *IEEE Access*, vol. 7, pp. 80043–80057, 2019.

[9] D. Wubben and Y. Lang, "Near-optimum power allocation for outage restricted distributed MIMO multi-hop networks," in *Proceedings of the 2008 IEEE Global Telecommunications Conference*, pp. 1–5, New Orleans, LO, USA, December 2009.

[10] A. Emir, H. Kaya, O. Erkaymaz, and E. Ozturk, "Optimum power allocation in amplify and forward relay selection systems by using ANNs," *Journal of Computing, Communications & Instrumentation Engg (IJCCIE)*, vol. 3, no. 2, 2016.

[11] C. Ling, X. Yin, S. R. Boque, and M. G. Lozanoe, ""Optimal power allocation and relay selection in spectrum sharing cooperative networks," A: URSI general assembly and scientific symposium," in *Proceedings of the 31st URSI General Assembly and Scientific Symposium*, Beijing, China, August 2014.

[12] G. Alirezaei, O. Taghizadeh, and R. Mathar, "Optimum power allocation in sensor networks for active radar applications," *IEEE Transactions on Wireless Communications*, vol. 14, no. 5, pp. 2854–2867, 2015.

[13] A. Benigno, P. Pangun, F. Carlo et al., "On power control for wireless sensor networks: system model, middleware component and experiment evaluation," in *Proceedings of the 2007 European Control Conference (ECC)*, Kos, Greece, July 2007.

[14] S. Lan, J. Li, C. Tan, Q. Chen, and J. Zhang, "Energy Efficient Network Strategy for Nanosatellites Cluster Flight Formations," 2013.

[15] R. Rajkumar, C. Lee, J. P. Lehoczky, and D. P. Siewiorek, "Practical solutions for QoS-based resource allocation problems," in *Proceedings of the IEEE Real-Time Systems Symposium*, Madrid, Spain, December 1998.

[16] J. P. Hansen, S. Ghosh, R. Rajkumar, and J. Lehoczky, "Resource management of highly configurable tasks," in *Proceedings of the 18th International Parallel and Distributed Processing Symposium*, Santa Fe, NM, USA, April 2004.

[17] R. Rajkumar, C. Lee, J. Lehoczky, and D. Siewiorek, "A resource allocation model for QoS management," in *Proceedings of the Real-Time Systems Symposium*, San Francisco, CA, USA, August 2002.

[18] J. P. Hansen, R. Rajkumar, J. Lehoczky, and S. Ghosh, "Resource Management for Radar Tracking," in *Proceedings of the 2006 IEEE Conference on Radar*, Verona, NY, USA, April 2006.

[19] J. P. Hansen, S. Hissam, and L. Wrage, "QoS optimization in ad hoc wireless networks through adaptive control of marginal utility," in *Proceedings of the 2013 IEEE Wireless Communications and Networking Conference (WCNC)*, pp. 1192–1197, Shanghai, China, April 2013.

[20] C. T. Van, E. Bjornson, and E. G. Larsson, "Joint power allocation and user association optimization for massive MIMO systems," *IEEE Transactions on Wireless Communications*, vol. 15, no. 9, pp. 6384–6399, 2016.

[21] W. Gao, L. Ma, and G. Chuai, "Energy efficient power allocation strategy for 5G carrier aggregation scenario," *EURASIP Journal on Wireless Communications and Networking*, vol. 2017, Article ID 140, 2017.

[22] D. Korpi, T. Riihonen, A. Sabharwal, and M. Valkama, "Transmit power optimization and feasibility analysis of self-backhauling full-duplex radio access systems," *IEEE Transactions on Wireless Communications*, vol. 17, no. 6, pp. 4219–4236, 2018.

[23] S. Dasgupta, G. Mao, and B. D. O. Anderson, "A new measure of wireless network connectivity," *IEEE Transactions on Mobile Computing*, vol. 14, no. 9, pp. 1765–1779, 2015.

[24] T. Yan, S. Hu, and J. Mo, "Path formation time in the noise-limited fractionated spacecraft network with FDMA," *International Journal of Aerospace Engineering*, vol. 2018, Article ID 9124132, 12 pages, 2018.

[25] F. G. Zimmerman and P. Gurfil, "Optimal target states for satellite cluster flight control on near-circular orbits," *Journal of Guidance, Control, and Dynamics*, vol. 38, no. 3, pp. 375–383, 2015.

[26] P. Medagliani, L. Consolini, and G. Ferrari, "An optimization-theoretic approach to transmit power control in wireless sensor network," 2020.

[27] T. Hmello and G. Bayraksan, "Monte Carlo sampling-based methods for stochastic optimization," *Surveys in Operations Research and Management Science*, vol. 19, no. 1, pp. 56–85, 2014.

[28] K. Hamed, G. Rosenberg, and G. K. Helmut, "Effective optimization using sample persistence: a case study on quantum annealers and various Monte Carlo optimization methods," *Physical Review*, vol. 96, no. 4, 2017.

[29] V. Bally, "The central limit theorem for a nonlinear algorithm based on quantization," *Proceedings of the Royal Society of London. Series A: Mathematical, Physical and Engineering Sciences*, vol. 460, no. 2041, pp. 221–241, 2004.

[30] A. Golkar, "Federated satellite systems (FSS): a vision towards an innovation in space systems design," in *Proceedings of the 9th IAA Symposium on Small Satellites for Earth Observation*, Berlin, Germany, 2013.

[31] D. Selva, A. Golkar, O. Korobova, I. L. I. Cruz, P. Collopy, and O. L. de Weck, "Distributed earth satellite systems: what is needed to move forward?" *Journal of Aerospace Information Systems*, vol. 14, no. 8, pp. 412–438, 2017.